iScience

CellPress
OPEN ACCESS

Article

IL-30 protects against sepsis-induced myocardial dysfunction by inhibiting pro-inflammatory macrophage polarization and pyroptosis

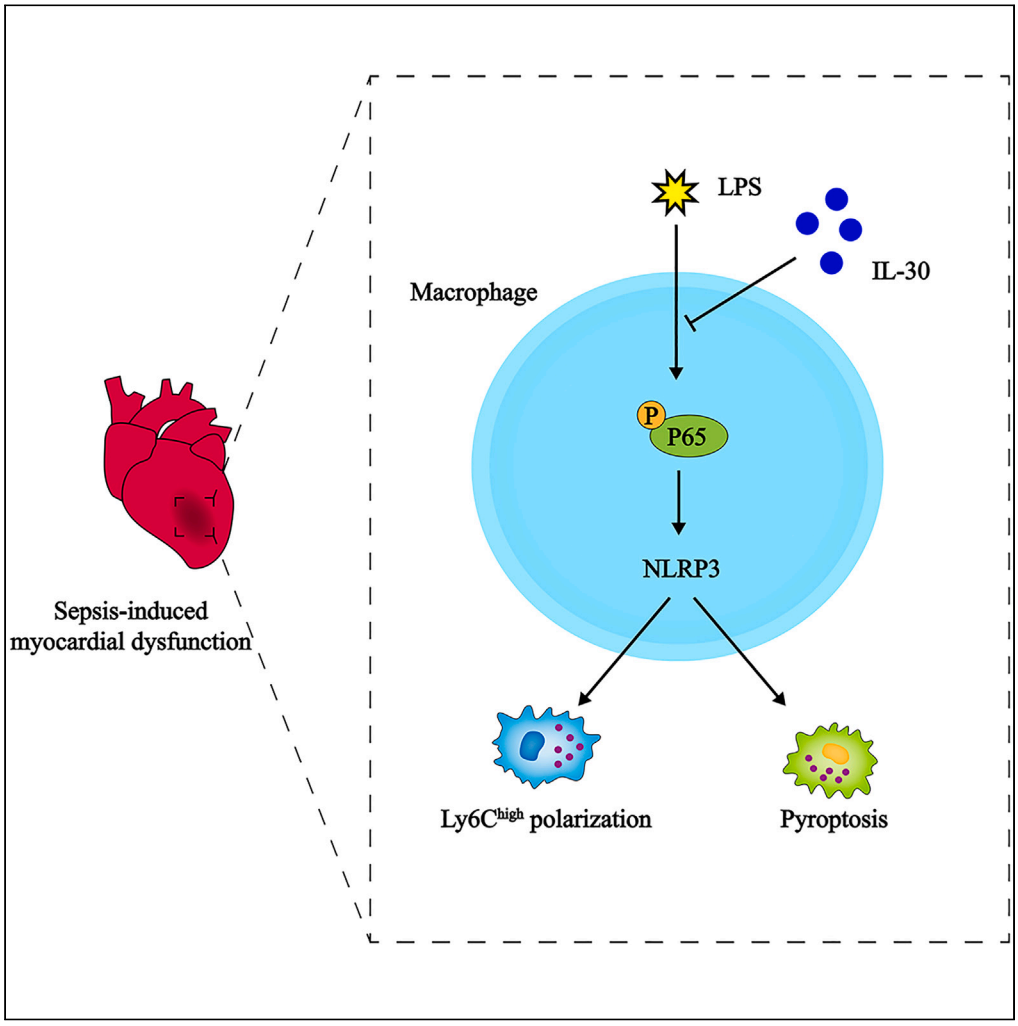

Mengmeng Zhao, Zihui Zheng, Pingan Zhang, ..., Cheng Wei, Jun Wan, Menglong Wang

wanjun@whu.edu.cn (J.W.)
whuwangmenglong@163.com (M.W.)

Highlights

IL-30 KO aggravates sepsis-induced cardiac dysfunction

IL-30 KO promotes LPS-induced Ly6C^{high} macrophage polarization and pyroptosis

The level of IL-30 is increased in sepsis patients and associated with the prognosis

Zhao et al., iScience 26, 107544
September 15, 2023
https://doi.org/10.1016/j.isci.2023.107544

iScience

CellPress
OPEN ACCESS

Article

IL-30 protects against sepsis-induced myocardial dysfunction by inhibiting pro-inflammatory macrophage polarization and pyroptosis

Mengmeng Zhao,[1,2,3,5] Zihui Zheng,[1,2,3,5] Pingan Zhang,[4,5] Yao Xu,[1,2,3] Jishou Zhang,[1,2,3] Shanshan Peng,[1,2,3] Jianfang Liu,[1,2,3] Wei Pan,[1,2,3] Zheng Yin,[1,2,3] Shuwan Xu,[1,2,3] Cheng Wei,[1,2,3] Jun Wan,[1,2,3,6,*] and Menglong Wang[1,2,3,*]

SUMMARY

Cardiac dysfunction is a well-recognized complication of sepsis and seriously affects the prognosis of sepsis patients. IL-30 has been reported to exert anti-inflammatory effects in various diseases. However, the role of IL-30 in sepsis-induced myocardial dysfunction (SIMD) remains unclear. Here, we explored the protective role of IL-30 in cecum ligation and puncture (CLP)-induced SIMD mice. IL-30 expression increased in the cardiac tissues of septic mice and was mainly derived from macrophages. IL-30 deletion or neutralization aggravated sepsis-induced cardiac dysfunction and injury, whereas recombinant IL-30 treatment significantly ameliorated it. Mechanistically, IL-30 deficiency exerts pro-inflammatory effects by promoting Ly6C^{high} macrophage polarization and pyroptosis. Inhibiting NLRP3 with MCC950 significantly reversed cardiac dysfunction, macrophage polarization and pyroptosis aggravated by IL-30 deficiency. Recombinant IL-30 inhibited pro-inflammatory macrophage polarization and pyroptosis *in vivo* and vitro. Taken together, these results suggest that IL-30 protects against SIMD by inhibiting pro-inflammatory macrophage polarization and pyroptosis.

INTRODUCTION

Sepsis is a clinical syndrome of multiple organ dysfunction caused by an uncontrollable infection-induced inflammatory response in the body. Sepsis has a high mortality rate, seriously threatens human health, and places a considerable economic burden on the public health system. Therefore, it is urgent to improve the success rate of sepsis treatment. Multiple organ failure is the leading cause of death in patients with sepsis, and the heart is one of the most vulnerable target organs. Sepsis-induced myocardial dysfunction (SIMD) is a partially reversible cardiac injury caused by sepsis. In patients with septic shock, the incidence of SIMD can reach 50% and, once the patient experiences cardiac dysfunction, the mortality rate can reach 70%.[1] Finding therapeutic strategies to alleviate SIMD has important clinical implications.

The pathophysiology and pathogenesis of SIMD are very complex and have not yet been fully elucidated. Unbalanced inflammatory responses are characteristically seen in sepsis and are abundant during the progression of SIMD. Bacterial lipopolysaccharide (LPS), endotoxin, and LPS-binding protein form immune complexes. Immune cells such as monocytes, macrophages, and lymphocytes recognize immune complexes on the surface of pathogens, activate intracellular signal transduction mechanisms, and synthesize and release a large number of cytokines, such as tumor necrosis factor alpha (TNF-α) and interleukin 6 (IL-6), causing cardiac injury.[2] Studies have found that TNF-α can cause myocardial injury by inhibiting calcium ion influx, activating proteolytic enzymes, and inducing oxidative stress and inflammatory responses.[3] Intraperitoneal injection of TNF-α in normal mice can cause decreased myocardial contractility and reversible left ventricular dilation.[3] Additionally, IL-6 decreases myocardial contractility by activating type 2 cyclooxygenase and nitric oxide synthase, and SIMD can be significantly alleviated by neutralizing IL-6.[4] Regulation of the inflammatory response is one of the potential strategies for the treatment of SIMD.

[1]Department of Cardiology, Renmin Hospital of Wuhan University, Wuhan 430060, P.R. China

[2]Cardiovascular Research Institute, Wuhan University, Wuhan 430060, P.R. China

[3]Hubei Key Laboratory of Cardiology, Wuhan 430060, P.R. China

[4]Department of Clinical Laboratory, Renmin Hospital of Wuhan University, Wuhan, P.R. China

[5]These authors contributed equally

[6]Lead contact

*Correspondence: wanjun@whu.edu.cn (J.W.), whuwangmenglong@163.com (M.W.)

https://doi.org/10.1016/j.isci.2023.107544

IL-30, a subunit of IL-27, was recently discovered to have IL27-independent biological functions. IL-30 is mainly derived from myeloid cells, including monocytes, macrophages and dendritic cells.[5] IL-30 can also be produced by microglia and astrocytes in the central nervous system, alveolar and interstitial macrophages in lung tissue, and Kupffer cells in the liver.[6] IL-30 has been reported to alleviate acute and chronic inflammation-induced liver damage by regulating T lymphocytes.[7–9] Additionally, it suppresses central nervous system autoimmunity by antagonizing Th1 and Th17 responses in experimental autoimmune uveitis.[10] Moreover, IL-30 ameliorates imiquimod and K14-VEGF-induced psoriasis-like disease by inhibiting innate and adaptive immune responses.[11] These limited *in vivo* studies suggest that IL-30 has anti-inflammatory effects in inflammatory diseases. This concept needs to be explored in other inflammatory disease models to better understand this effect and the underlying mechanisms.

We hypothesized that IL-30 protects mice from systemic inflammation, cardiac dysfunction and sepsis-induced death. Using a cecum ligation and puncture (CLP)-induced sepsis model, we identified a novel function of IL-30 in SIMD and its associated mechanisms.

RESULTS

IL-30 expression was upregulated in mice with sepsis

To explore the possible involvement of IL-30 in SIMD, we first detected expression levels of IL-30 in heart tissues from CLP-treated mice. The mRNA and protein levels of IL-30 were both upregulated in cardiac tissues of septic mice (Figures 1A and 1B). The results of immunofluorescence staining further showed that the expression of IL-30 in the heart was significantly increased after CLP (Figure 1C). Compared to sham mice, the ratio of IL-30 positive cells in the cardiac tissues was upregulated in septic mice (Figure 1D). In addition, IL-30 primarily was derived from $CD45^+$ immune cells (Figure 1E). Further clustering results indicated that IL-30 was mainly expressed in $CD45^+CD11B^+F4/80^+$ macrophages (about 84.7%) and $CD45^+CD3^+$ T cells (about 13.7%) in the heart (Figure 1E). The results of immunofluorescence staining further confirmed the expression of IL-30 in macrophages in cardiac tissues (Figure S1).

IL-30 deletion aggravates sepsis-induced cardiac dysfunction and injury

IL-30 knockout (KO) mice and C57 mice (WT) were purchased to explore the role of IL-30 in sepsis-induced cardiac injury (Figures 2A and 2B). IL-30 depletion significantly aggravated sepsis-induced mortality (Figure 2C). IL-30 deficiency aggravated sepsis-induced cardiac dysfunction, as shown by echocardiography (Figure 2D and Table S1). IL-30 knockout further increased the expression levels of biomarkers for cardiac injury, including creatine kinase-myocardial band (CK-MB) and lactate dehydrogenase (LDH), in the cardiac tissue and serum of septic mice, suggesting that IL-30 depletion aggravated sepsis-induced cardiac injury (Figures 2E–2H). Western blotting results indicated that CLP treatment inhibited the expression of B-cell lymphoma-2 (BCL2) but increased the expression of BCL2-associated X (BAX) and cleaved caspase3 (c-caspase3) (Figure 2I). IL-30 depletion further exaggerated these results, suggesting that IL-30 depletion aggravates sepsis-induced cardiomyocyte apoptosis. Taken together, IL-30 deficiency aggravates sepsis-induced cardiac dysfunction and injury.

In addition, CLP treatment produced significant pathological changes in lung, including alveolar hemorrhage and massive inflammatory cell infiltration, while IL-30 knockout mice suffered greater trauma (Figures S2A and S2B). Furthermore, IL-30 deletion significantly aggravated CLP-induced pulmonary edema as evidenced by protein leakage in bronchoalveolar lavage fluid (BALF) (Figure S2C). Serum urea and creatinine were significantly elevated in CLP-treated mice compared with sham mice, which were further exacerbated by IL-30 depletion (Figures S2D and S2E). In addition, IL-30 deficiency significantly increased serum alanine aminotransferase (ALT) and aspartate aminotransferase (AST) levels in sepsis mice (Figures S2F and S2G). Taken together, IL-30 depletion exacerbated sepsis-induced target organs damage, including lung, kidney, and liver.

IL-30 knockout aggravates sepsis-induced inflammatory responses in the heart by promoting proinflammatory macrophage polarization and pyroptosis

The cardiac mRNA expression of proinflammatory cytokines, such as IL-1β, IL-6 and tumor necrosis factor alpha (TNF-α), and chemokines, such as monocyte chemoattractant protein-1 (MCP-1) and C-X-C motif chemokine 2 (CXCL2), was increased in septic mice, and IL-30 deficiency further promoted the expression of these cytokines and chemokines (Figures 3A–3E). Flow cytometry results suggested that IL-30 depletion

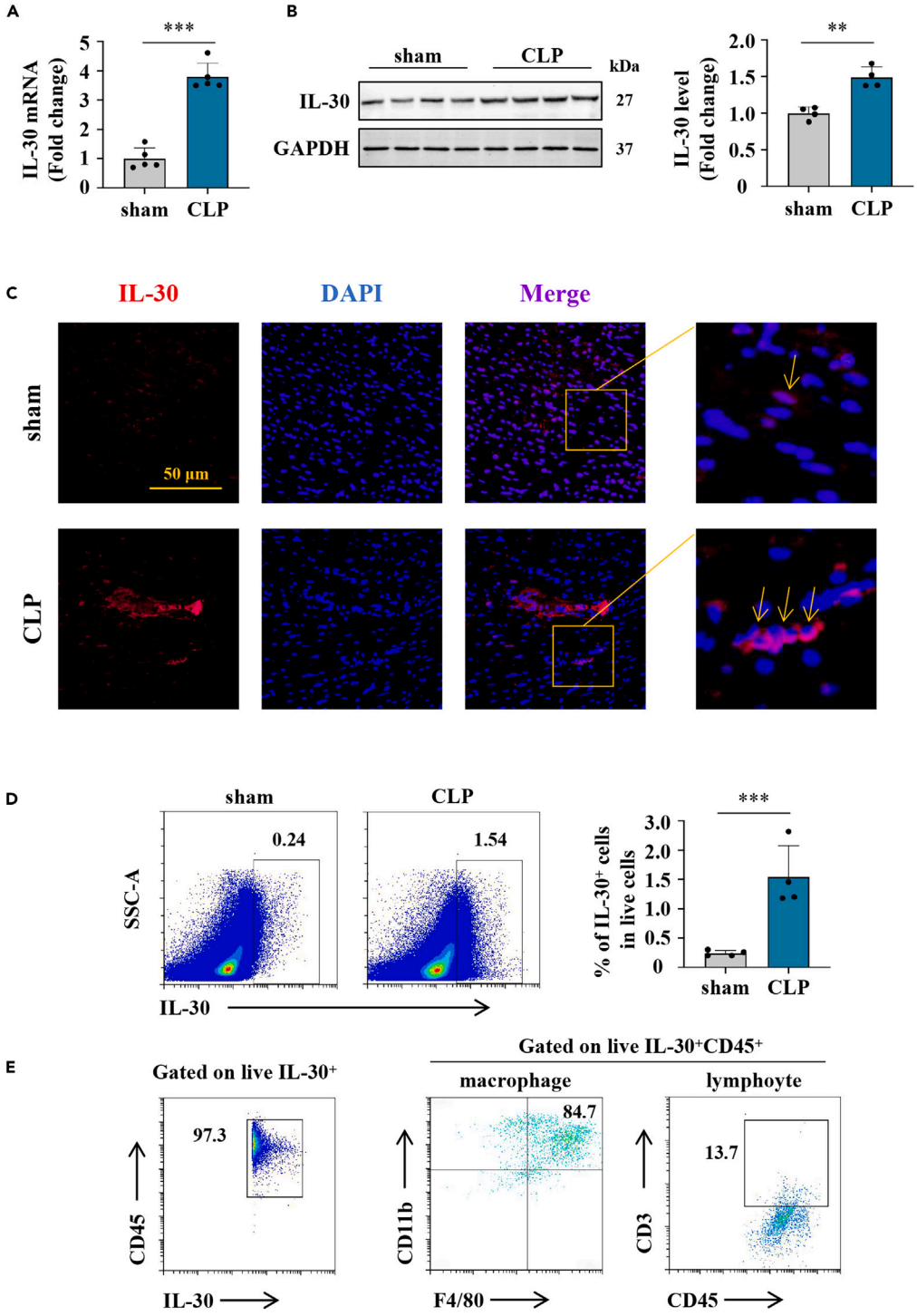

Figure 1. IL-30 expression was upregulated in mice with sepsis

(A) The IL-30 mRNA levels (n = 5).

(B) The IL-30 protein levels (n = 4).

(C) Representative immunofluorescence staining images of cardiac tissues for IL-30 (n = 4).

(D and E) The source of cardiac IL-30 in septic mice (n = 4). Values represent the mean +SEM. * indicates $p < 0.05$, ** indicates $p < 0.01$, *** indicates $p < 0.001$. IL-30, interleukin 30.

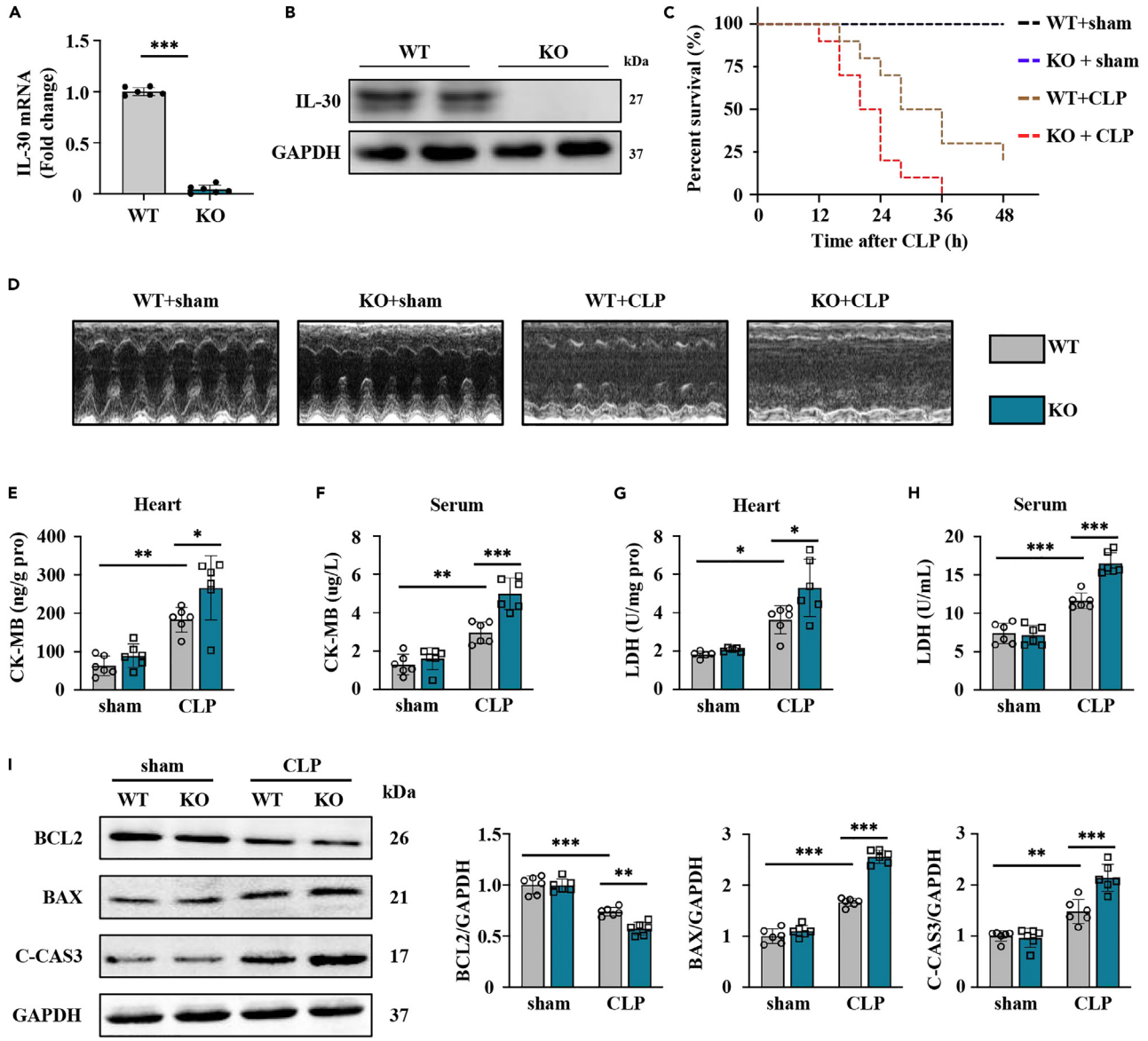

Figure 2. IL-30 deletion aggravates sepsis-induced cardiac dysfunction and myocardial injury

(A and B) mRNA and protein levels of cardiac tissue IL-30 (n = 6).

(C) Survival rate (n = 10).

(D) Representative echocardiographic images (n = 4).

(E–H) The cardiac and serum levels of CK-MB and LDH (n = 6).

(I) Representative immunoblots and corresponding quantification showing cardiac tissue levels of BAX, BCL2 and c-caspase3 (n = 6). Values represent the mean ± SEM. * indicates $p < 0.05$, ** indicates $p < 0.01$, *** indicates $p < 0.001$. IL-30, interleukin 30; CK-MB, creatine kinase-myocardial band; LDH, lactate dehydrogenase; BCL2, B-cell lymphoma-2; BAX, BCL2-Associated X.

aggravated sepsis-induced cardiac macrophage infiltration (Figure 3F). Additional typing of macrophages revealed that IL-30 depletion promoted sepsis-induced infiltration of $F4/80^{+}Ly6C^{high}$ macrophages (Figure 3G). IL-30 depletion promoted sepsis-induced expression of CD80, CD86, and inducible nitric oxide synthase (INOS) (proinflammatory macrophage biomarkers) and further suppressed the expression of CD163 and CD206 (anti-inflammatory macrophage biomarkers) (Figures 3H and 3I). The results of immunofluorescence staining showed that IL-30 deficiency increased the ratio of $F4/80^{+}caspase1^{+}$ macrophages in septic mice, suggesting aggravated macrophage pyroptosis (Figure 3J). The levels of NOD-like receptor thermal protein domain associated protein 3 (NLRP3), IL-1β, IL-18 and N-terminal gasdermin

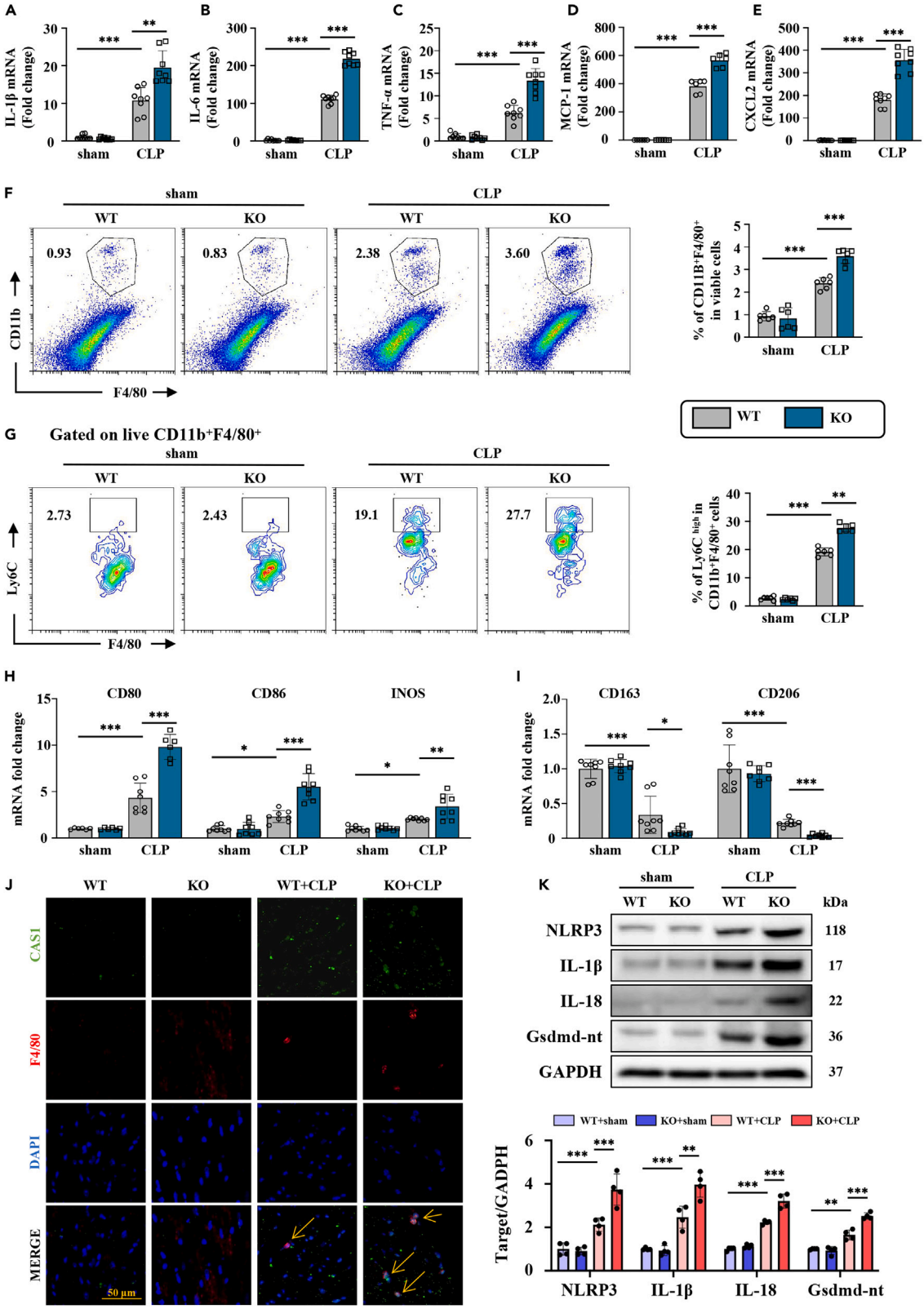
A
IL-1β mRNA (Fold change)
B
IL-6 mRNA (Fold change)
C
TNF-α mRNA (Fold change)
D
MCP-1 mRNA (Fold change)
E
CXCL2 mRNA (Fold change)
sham
CLP
F
WT
KO
0.93
0.83
2.38
3.60
CD11b
F4/80
% of CD11B+F4/80+ in viable cells
G
Gated on live CD11b+F4/80+
2.73
2.43
19.1
27.7
Ly6C
% of Ly6C high in CD11b+F4/80+ cells
H
CD80
CD86
INOS
mRNA fold change
I
CD163
CD206
J
WT
KO
WT+CLP
KO+CLP
CAS1
F4/80
DAPI
MERGE
50 μm
K
kDa
NLRP3
IL-1β
IL-18
Gsdmd-nt
GAPDH
WT+sham
KO+sham
WT+CLP
KO+CLP
Target/GADPH

Figure 3. IL-30 knockout aggravates sepsis-induced inflammatory responses in the heart by promoting proinflammatory macrophage polarization and pyroptosis

(A–E) The cardiac mRNA levels of IL-1β, IL-6, TNF-α, MCP-1 and CXCL2 in each group (n = 8).

(F) Representative flow cytometry images and corresponding quantification showing the ratio of $CD11B^{+}$ $F4/80^{+}$ macrophages in each group (n = 6).

(G) Representative flow cytometry images and corresponding quantification showing the ratio of $F4/80^{+}Ly6C^{high}$ macrophages in each group (n = 6).

(H) mRNA levels of CD80, CD86 and INOS in each group (n = 8).

(I) mRNA levels of CD163 and CD206 in each group (n = 8).

(J) Representative immunofluorescence staining images for F4/80 and caspase1 (n = 4).

(K) Representative immunoblots and corresponding quantification showing cardiac tissue levels of NLRP3, IL-1β, IL-18 and GSDMD-nt (n = 4). Values represent the mean ± SEM. * indicates $p < 0.05$, ** indicates $p < 0.01$, *** indicates $p < 0.001$. IL, interleukin; MCP-1, monocyte chemoattractant protein-1; CXCL2, C-X-C motif chemokine 2; INOS, inducible nitric oxide synthase; NLRP3, NOD-like receptor thermal protein domain associated protein 3; caspase 1, cysteinyl aspartate specific proteinase-1; GSDMD-nt, N-terminal gasdermin domain-containing protein 1.

domain-containing protein 1 (GSDMD-nt) were also upregulated by IL-30 depletion in septic mice (Figure 3K). These results suggest that IL-30 knockout aggravates sepsis-induced inflammatory responses in the heart by promoting proinflammatory macrophage polarization and pyroptosis.

Neutralization of IL-30 aggravates cardiac dysfunction by promoting proinflammatory macrophage polarization and pyroptosis

To further confirm the biological relevance of IL-30 during sepsis, we used a neutralizing polyclonal antibody against IL-30 in septic mice. Treatment with anti-mouse IL-30 antibody significantly exacerbated cardiac dysfunction in septic mice compared with normal IgG (Figure S3A). IL-30 neutralization did not affect the level of macrophage polarization in sham mice, but promoted pro-inflammatory macrophage polarization in the hearts of septic mice (Figures S3B and S3C). Neutralization of IL-30 aggravated the expression levels of proinflammatory cytokines (IL-6 and TNF-α) and markers of pro-inflammatory macrophage polarization (INOS) in the heart of septic mice (Figures S3D–S3F). Meanwhile, IL-30 neutralization promoted the expression of pyroptosis-related proteins in cardiac tissue of septic mice, including NLRP3, cleaved caspase1, IL-1β and GSDMD-nt (Figure S3G). These results suggest that neutralization of IL-30 exacerbates sepsis-induced cardiac dysfunction, macrophage polarization, and pyroptosis.

Transplantation of IL-30-deficient bone marrow cells aggravates SIMD in WT mice

Bone marrow transplantation was used to explore the role of bone marrow cell-derived IL-30 in SIMD. Clodronate liposomes were first used to clear macrophages in WT mice and verified by flow cytometry (Figure S4A). Bone marrow cells were then extracted from WT mice and IL-30 KO mice and reinfused into WT mice via tail vein injection (Figure S4B). We treated mice after bone marrow transplantation with CLP and found that septic mice transplanted with KO bone marrow cells had significantly aggravated cardiac dysfunction (Figure S4C). KO bone marrow transplantation promoted pro-inflammatory macrophage polarization and increased IL-6 expression in the heart of septic mice (Figures S4D and S4E). KO bone marrow transplantation also promoted the expression of NLRP3, cleaved caspase1, IL-1β and GSDMD-nt in the hearts of septic mice (Figure S4F). Taken together, these results suggest that bone marrow cells-derived IL-30 is involved in sepsis-induced SIMD.

IL-30 deficiency promoted LPS-induced proinflammatory macrophage polarization and pyroptosis *in vitro*

Bone marrow-derived macrophages (BMDMs) from WT and KO mice were used to explore the role of IL-30 *in vitro*. IL-30 deficiency significantly promoted LPS-induced $Ly6C^{high}$ macrophage polarization (Figure 4A). The mRNA expression of IL-6, TNF-α and biomarkers for proinflammatory macrophage polarization (CD80 and CD86) were upregulated by IL-30 deficiency (Figures 4B–4D). In addition, IL-30 depletion also increased the level of NLRP3, cleaved-caspase1, IL-1β and GSDMD-nt after LPS treatment, suggesting aggravated macrophage pyroptosis (Figure 4E). Taken together, these results showed that IL-30 deficiency promoted LPS-induced proinflammatory macrophage polarization and pyroptosis *in vitro*.

Inhibiting NLRP3 with MCC950 blocked proinflammatory macrophage polarization and pyroptosis induced by IL-30 deficiency

MCC950 is a specific small-molecule inhibitor that selectively blocks activation of the NLRP3 inflammasome.[12] Inhibiting NLRP3 with MCC950 treatment significantly attenuated IL-30 deficiency aggravated cardiac dysfunction and cardiac injury in mice with sepsis (Figures 5A–5C). MCC950 treatment also reduced the mRNA level of IL-6 and TNF-α in KO mice with sepsis (Figure 5D). The ratio of $Ly6C^{high}$

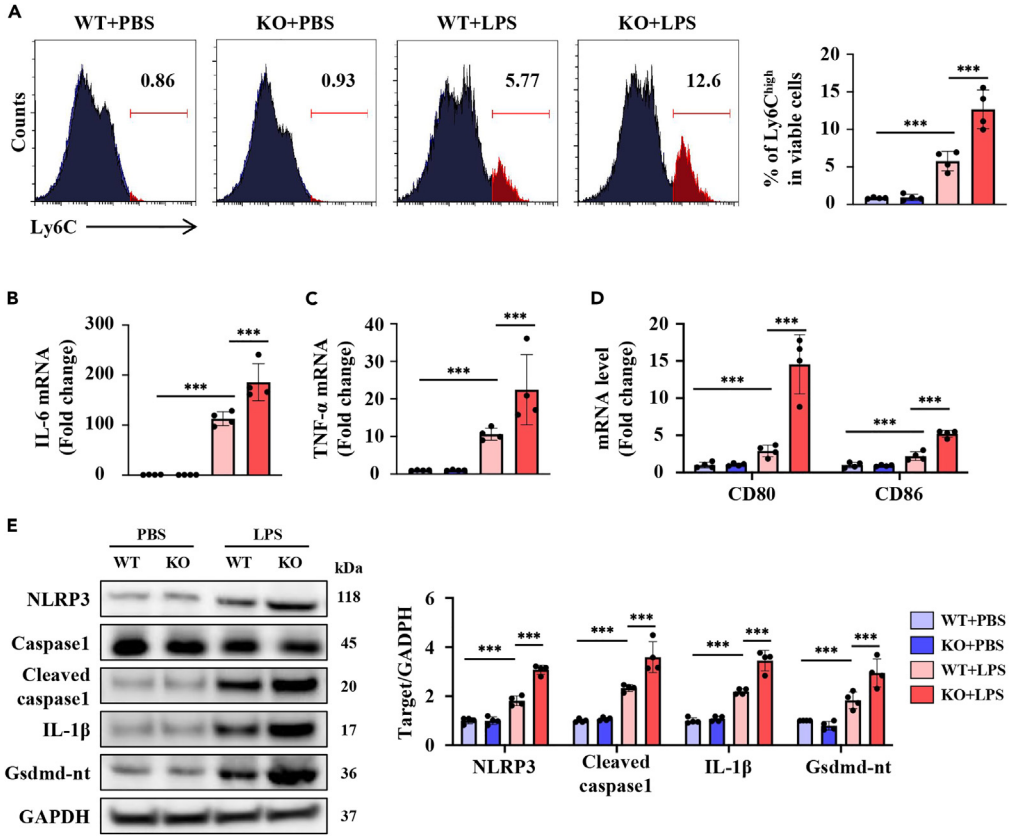

Figure 4. IL-30 deficiency promoted LPS-induced proinflammatory macrophage polarization and pyroptosis *in vitro*

(A) Representative flow cytometry images and corresponding quantification showing the ratio Ly6C^{high} macrophages in each group (n = 4).

(B–D) mRNA level of IL-6, TNF-α, CD80 and CD86 (n = 4).

(E) Representative immunoblots and corresponding quantification showing levels of NLRP3, caspase1, IL-1β and GSDMD-nt (n = 4). Values represent the mean ± SEM. * indicates $p < 0.05$, ** indicates $p < 0.01$, *** indicates $p < 0.001$. IL, interleukin; NLRP3, NOD-like receptor thermal protein domain associated protein 3; caspase 1, cysteinyl aspartate specific proteinase-1; GSDMD-nt, N-terminal gasdermin domain-containing protein 1.

macrophages in the heart of KO mice with sepsis was significantly reduced by MCC950 (Figure 5E). In addition, MCC950 treatment ameliorated pyroptosis in KO mice with sepsis as shown by the level of cleaved-caspase1, IL-1β and GSDMD-nt (Figure 5F). *In vitro*, MCC950 treatment inhibited Ly6C^{high} macrophages polarization in LPS treated KO BMDMs (Figure 5G). The mRNA levels of IL-6 and INOS were also reduced by MCC950 treatment (Figure 5H). MCC950 treatment significantly inhibited IL-30 deficiency promoted macrophage pyroptosis (Figure 5I). Taken together, these results suggested that inhibiting NLRP3 with MCC950 blocked proinflammatory macrophage polarization and pyroptosis induced by IL-30 deficiency *in vivo* and vitro.

Recombinant IL-30 attenuates sepsis-induced cardiac dysfunction and injury by inhibiting proinflammatory macrophage polarization and pyroptosis

Since IL-30 is a subunit of IL-27, mice deficient in IL-30 also lack functional IL-27. We administered recombinant IL-27 or IL-30 to IL-30 KO mice to explore the mechanism by which IL-30 deletion aggravates SIMD. Compared to KO mice with sepsis, IL30 but not IL-27 treatment significantly improved sepsis-induced cardiac dysfunction and injury (Figures S5A and S5B). In addition, IL-27 treatment exacerbated and IL-30 attenuated cardiac inflammatory responses in septic KO mice, as shown by the mRNA expression of IL-6 and TNF-α (Figures S5C and S5D). These data suggest that IL-30 deficiency is mainly involved in the regulation of SIMD by affecting the expression level of IL-30.

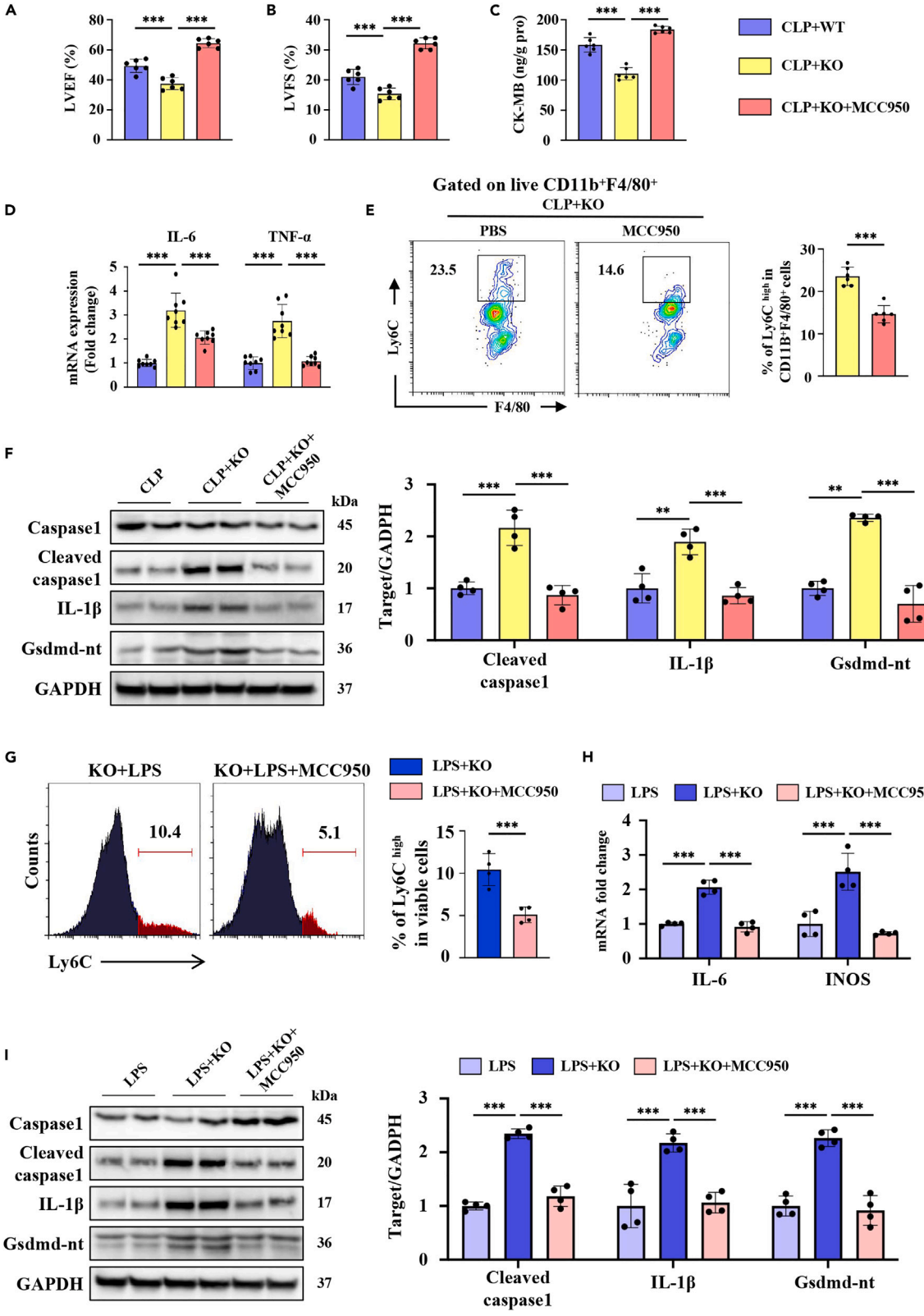
A
LVEF (%)
B
LVFS (%)
C
CK-MB (ng/g pro)
CLP+WT
CLP+KO
CLP+KO+MCC950
D
IL-6
TNF-α
mRNA expression (Fold change)
E
Gated on live CD11b+F4/80+
CLP+KO
PBS
MCC950
23.5
14.6
Ly6C
F4/80
% of Ly6C high in CD11B+F4/80+ cells
F
CLP
CLP+KO
CLP+KO+ MCC950
kDa
Caspase1
Cleaved caspase1
IL-1β
Gsdmd-nt
GAPDH
45
20
17
36
37
Target/GADPH
Cleaved caspase1
IL-1β
Gsdmd-nt
G
KO+LPS
KO+LPS+MCC950
10.4
5.1
Counts
Ly6C
LPS+KO
LPS+KO+MCC950
% of Ly6C high in viable cells
H
LPS
LPS+KO
LPS+KO+MCC950
mRNA fold change
IL-6
INOS
I
LPS
LPS+KO
LPS+KO+ MCC950
kDa
Caspase1
Cleaved caspase1
IL-1β
Gsdmd-nt
GAPDH
45
20
17
36
37
Target/GADPH
Cleaved caspase1
IL-1β
Gsdmd-nt

Figure 5. Inhibiting NLRP3 with MCC950 blocked proinflammatory macrophage polarization and pyroptosis induced by IL-30 deficiency

(A and B) LVEF and FS (n = 6).

(C) Cardiac CK-MB (n = 6).

(D) mRNA level of IL-6 and TNF-α (n = 8).

(E) Representative flow cytometry images and corresponding quantification showing the ratio of $F4/80^{+}Ly6C^{high}$ macrophages in each group (n = 6).

(F) Representative immunoblots and corresponding quantification showing cardiac tissue levels of caspase1, IL-1β and GSDMD-nt (n = 4).

(G) Representative flow cytometry images and corresponding quantification showing the ratio of $Ly6C^{high}$ macrophages in each group (n = 4).

(H) mRNA level of IL-6 and INOS (n = 4).

(I) Representative immunoblots and corresponding quantification showing levels of caspase1, IL-1β and GSDMD-nt (n = 4). Values represent the mean ± SEM. * indicates $p < 0.05$, ** indicates $p < 0.01$, *** indicates $p < 0.001$. IL, interleukin; CK-MB, creatine kinase-myocardial band; caspase 1, cysteinyl aspartate specific proteinase-1; GSDMD-nt, N-terminal gasdermin domain-containing protein 1.

We next explored the protective effect of recombinant IL-30 in septic mice. IL-30 treatment reduced mortality from sepsis (Figure 6A). IL-30 treatment significantly improved cardiac dysfunction in septic mice, as shown by echocardiography (Figure 6B). Furthermore, IL-30 significantly attenuated sepsis-induced cardiac injury (Figures 6C–6F). IL-30 attenuated sepsis-induced expression of proinflammatory cytokines and chemokines (Figures 6G–6J). IL-30 treatment inhibited sepsis-induced infiltration of macrophages in the heart and reduced the proportion of $Ly6C^{high}$ macrophages (Figure 6K). IL-30 inhibited the LPS-induced expression of CD80, CD86 and INOS and restored the expression of CD163 and CD206 (Figures 6L and 6M). In addition, IL-30 treatment significantly inhibited the levels of NLRP3, cleaved-caspase1, IL-1β and IL-18 in septic mice (Figure 6N). These results suggest that IL-30 ameliorated sepsis-induced cardiac dysfunction by inhibiting proinflammatory macrophage polarization and pyroptosis.

IL-30 inhibited proinflammatory macrophage polarization and pyroptosis *in vitro*

BMDMs from WT mice were used to examine the role of IL-30 on macrophage polarization and pyroptosis. Recombinant IL-30 reduced the ratio of $Ly6C^{high}$ macrophages after LPS treatment (Figure 7A). IL-30 also reduced the mRNA level of IL-6 and INOS in BMDMs treated with LPS (Figure 7B). In addition, IL-30 significantly reduced the expression of NLRP3, caspase1, IL-1β and IL-18 in BMDMs with LPS (Figure 7C). These results suggested that IL-30 inhibited pro-inflammatory macrophage polarization and pyroptosis *in vitro*. To further explore the mechanism(s) how IL-30 upregulates NLRP3, we examined the expression of JAK/STAT and MAPK signaling in IL-30-treated BMDMs. IL-30 had no significant effect on the phosphorylation levels of JAK1, JAK2, STAT1 and STAT3 (Figure 7D). And the phosphorylation level of P38 and P65 were inhibited by IL-30, while the phosphorylation levels of ERK and JNK were not significantly changed (Figure 7D). We also examined the levels of these proteins in mouse hearts. IL-30 KO significantly increased the levels of phosphorylated P65 and P38 in the hearts of septic mice, which were downregulated by IL-30 (Figure S6). These results suggested that IL-30 may inhibited the P65 and P38 signal.

The serum levels of IL-30 were increased in sepsis patients

To translate our preclinical findings to humans, we collected plasma from sepsis and non-sepsis patients in the intensive care unit (ICU), as well as from healthy controls. We investigated the association between IL-30 plasma levels and sepsis outcomes, sequential organ failure assessment (SOFA). Patient demographics and clinical data are shown in Table S2. Our data showed that IL-30 plasma levels were 0.96-fold higher in sepsis patients than that in non-sepsis patients and 1.09-fold higher than that in healthy controls (Figure 8A). The patients with sepsis were further divided into three groups according to the SOFA score (interquartile range, S1: <3 points, S2: 3–9 points, S3: >9 points). Sepsis patients with higher SOFA scores had higher IL-30 levels (Figure 8B). When comparing the correlation of IL-30 levels with other indicators, including IL-6, AST, ALT, urea, creatinine, pro BNP (pro-brain natriuretic peptide), cTNI (cardiac troponin I), CK-MB and APTT (activated partial thromboplastin time), we found that elevated IL-30 plasma levels in sepsis patients correlated with higher IL-6 and CK-MB levels significantly (Figures 8C–8K). We investigated whether plasma IL-30 levels could serve as a predictor of 28-day mortality after admission in patients with sepsis. We found that IL-30 levels were 0.5-fold higher in non-survivors than in ICU non-septic patients and 1.0-fold higher in survivors (Figure 8L). Receiver operating curve (ROC) analysis comparing survivors with non-survivors demonstrated a strong specificity (91.04%, sensitivity 84.85%) for IL-30 plasma levels greater than 963.4 pg/L, indicating that IL-30 can be a valid predictor of mortality (Figure 8M).

DISCUSSION

In the present study, we found that serum IL-30 levels in sepsis patients were increased and correlated with patient prognosis and cardiac injury. The expression of IL-30 was increased in the cardiac tissue of septic

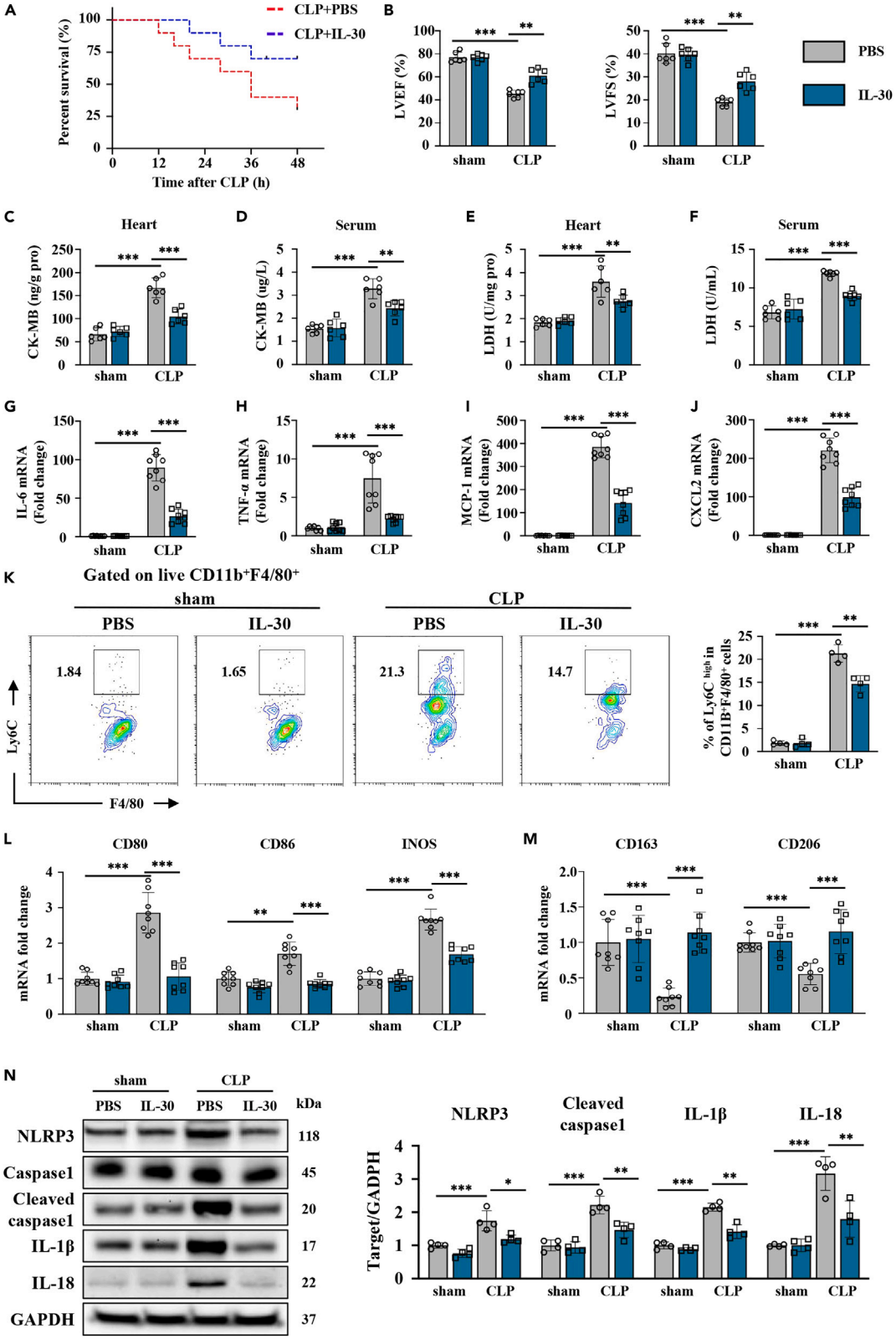
A
CLP+PBS
CLP+IL-30
Percent survival (%)
Time after CLP (h)
B
LVEF (%)
LVFS (%)
sham
CLP
PBS
IL-30
C
Heart
CK-MB (ng/g pro)
D
Serum
CK-MB (ug/L)
E
Heart
LDH (U/mg pro)
F
Serum
LDH (U/mL)
G
IL-6 mRNA (Fold change)
H
TNF-α mRNA (Fold change)
I
MCP-1 mRNA (Fold change)
J
CXCL2 mRNA (Fold change)
K
Gated on live CD11b+F4/80+
sham
CLP
PBS
IL-30
1.84
1.65
21.3
14.7
Ly6C
F4/80
% of Ly6C high in CD11B+F4/80+ cells
L
CD80
CD86
INOS
mRNA fold change
M
CD163
CD206
N
kDa
NLRP3
Caspase1
Cleaved caspase1
IL-1β
IL-18
GAPDH
118
45
20
17
22
37
Target/GADPH

Figure 6. Recombinant IL-30 attenuates sepsis-induced cardiac dysfunction and injury by inhibiting proinflammatory macrophage polarization and pyroptosis

(A) Survival rate (n = 10).
(B) Cardiac function (n = 6).
(C–F) The cardiac and serum levels of CK-MB and LDH were measured in each group (n = 6).
(G–J) mRNA level of IL-6, TNF-α, MCP-1 and CXCL2 (n = 8).
(K) Representative flow cytometry images and corresponding quantification showing the ratio of $F4/80^{+}Ly6C^{high}$ macrophages in each group (n = 4).
(L) mRNA levels of CD80, CD86 and INOS in each group (n = 8).
(M) mRNA levels of CD163 and CD206 in each group (n = 8).
(N) Representative immunoblots and corresponding quantification showing levels of NLRP3, caspase1, IL-1β and IL-18 (n = 4). Values represent the mean ± SEM. * indicates $p < 0.05$, ** indicates $p < 0.01$, *** indicates $p < 0.001$. IL, interleukin; CK-MB, creatine kinase-myocardial band; LDH, lactate dehydrogenase; MCP-1, monocyte chemoattractant protein-1; CXCL2, C-X-C motif chemokine 2; INOS, inducible nitric oxide synthase; NLRP3, NOD-like receptor thermal protein domain associated protein 3; caspase 1, cysteinyl aspartate specific proteinase-1.

mice. In addition, IL-30 was mainly expressed in macrophages in cardiac tissues. IL-30 knockout or neutralization aggravated sepsis-induced cardiac dysfunction and injury by promoting $Ly6C^{high}$ macrophage polarization and pyroptosis. Transplantation of IL-30-deficient bone marrow cells aggravated SIMD in WT mice. IL-30 deficiency promoted BMDMs proinflammatory polarization and pyroptosis *in vitro*. Inhibiting NLRP3 with MCC950 blocked proinflammatory macrophage polarization and pyroptosis induced by IL-30 deficiency. Recombinant IL-30 treatment ameliorated sepsis-induced cardiac injury by inhibiting $Ly6C^{high}$ macrophage polarization. Similarly, IL-30 inhibited LPS-induced $LY6G^{high}$ macrophage polarization and pyroptosis *in vitro*. Taken together, these results suggest that IL-30 protected against SIMD by inhibiting pro-inflammatory macrophage polarization and macrophage pyroptosis.

The serum level of IL-30 has been reported to be increased in septic patients and mice.[8,13,14] In this study, we also found IL-30 expression was upregulated in patients and mice with sepsis. IL-30 production during endotoxic shock and polymicrobial sepsis induced by CLP is partly dependent on tyrosine kinase 2 via an autocrine type I interferon (IFN) loop.[13] LPS-stimulated and IFN-gamma-induced IL-30 production were both dependent on the Toll-like receptor 4/myeloid differentiation factor 88-mediated pathway.[15] The potent anti-inflammatory function of IL-30 was first reported in a cytokine-induced liver injury model.[7] Exogenous IL-30 supplementation can alleviate CCl4-induced liver fibrosis or IL-12-induced liver toxicity by inhibiting IFN-γ expression, which is independent of IL27 and IL-27Rα.[9] IL-30 also attenuates experimental sepsis-induced liver injury by modulating NKT-cell cytokine profiles.[8] Our study is the first to find that serum levels of IL-30 are elevated in patients with sepsis and are associated with patient prognosis and cardiac injury. In addition, IL-30 can ameliorate sepsis-induced myocardial injury by regulating macrophage polarization and pyroptosis.

Macrophages are one of the most important innate immune cells and are antigen-delivering cells with high plasticity. Not only can macrophages recognize stimuli in the microenvironment to initiate innate immune responses, but they can also regulate host immune responses through differential polarization in response to changes in the microenvironment. Under the influence of different microenvironmental factors, macrophages can be transformed into a variety of different functional phenotypes. The two most important functional phenotypes are proinflammatory ($Ly6C^{high}$) and anti-inflammatory macrophages ($Ly6C^{low}$).[16] Studies have shown that macrophage polarization plays an important role in regulating immune homeostasis and inflammatory responses in patients with sepsis.[17] In the early stages of sepsis, proinflammatory factors such as IFN-γ and LPS induce macrophage polarization toward $Ly6C^{high}$ macrophages.[18] The number of $Ly6C^{high}$ macrophages continues to increase and release a large number of cytokines that cause severe inflammatory responses, such as IL-1, TNF-α, and IL-6.[19] $Ly6C^{high}$ macrophages have strong cytotoxic activity to kill pathogens and clear abnormal endogenous tissues and cells in the immune microenvironment. However, sustained $Ly6C^{high}$ macrophage polarization can lead to multiple organ and tissue damage, including myocardial tissue.[20] Inhibition of proinflammatory macrophage polarization and/or enhancement of anti-inflammatory macrophage polarization through different pathways can significantly improve septic myocardial injury.[21–24] Therefore, macrophage polarization is a key factor in the occurrence and development of cardiac injury in sepsis, and finding key targets to regulate macrophage polarization is of great significance to improve myocardial injury in sepsis. In our study, we found for the first time that IL-30 ameliorated septic myocardial injury by regulating macrophage polarization, which has important clinical value.

Recently, the pyroptosis of macrophage has also been highlighted in sepsis-related cardiac injury. Pyroptosis is a caspase-1-dependent proinflammatory cell death type.[25] Caspase1 activated by inflammasomes

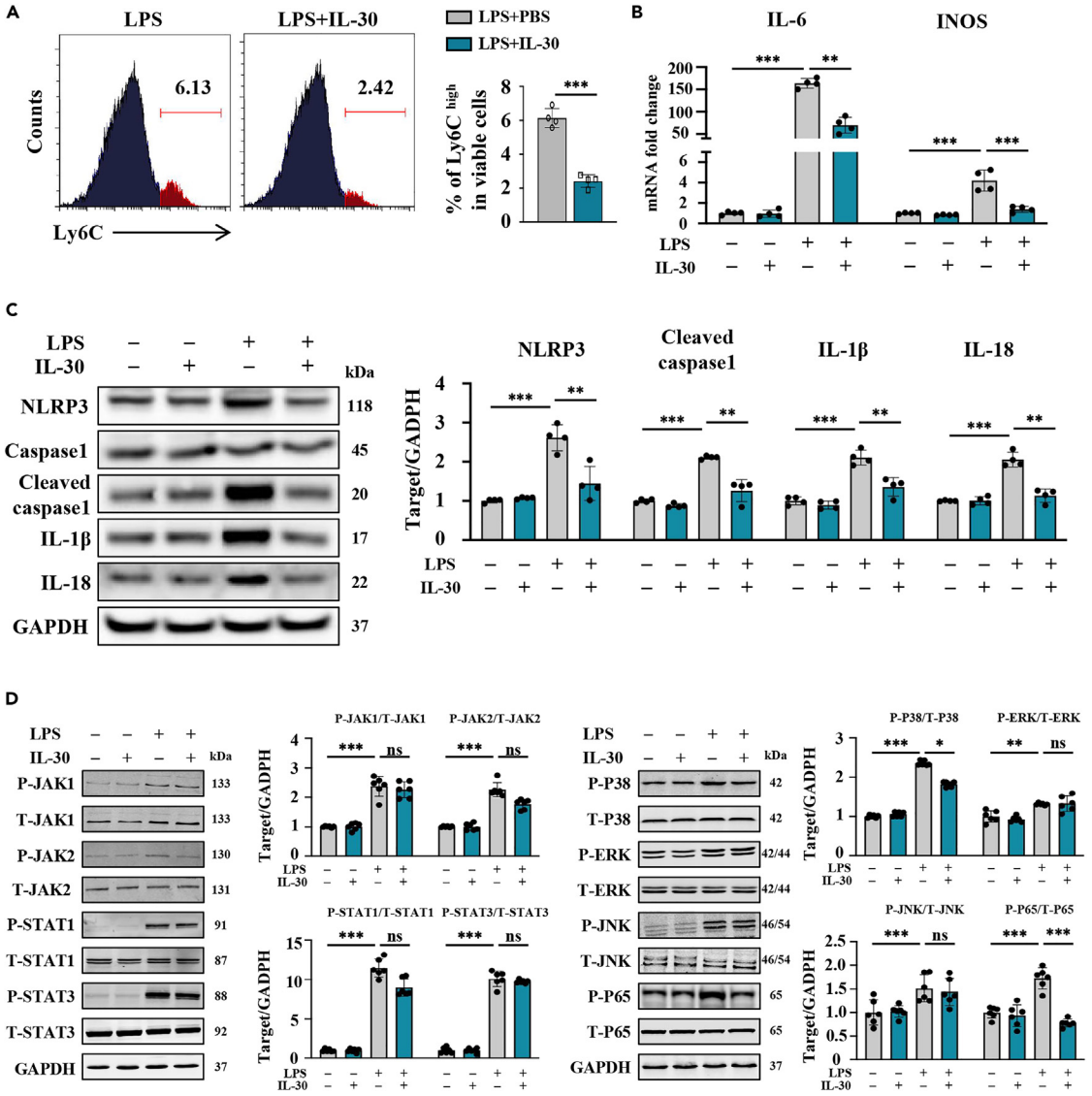

Figure 7. IL-30 inhibited proinflammatory macrophage polarization and pyroptosis *in vitro*

(A) Representative flow cytometry images and corresponding quantification showing the ratio of Ly6C^{high} macrophages in each group (n = 4).

(B) mRNA levels of IL-6 and INOS (n = 4).

(C) Representative immunoblots and corresponding quantification showing levels of NLRP3, caspase1, IL-1β and IL-18 (n = 4).

(D) Representative immunoblots and corresponding quantification showing levels of JAK1, JAK2, STAT1, STAT3, P38, ERK, JNK and P65 (n = 6). Values represent the mean ± SEM. * indicates $p < 0.05$, ** indicates $p < 0.01$, *** indicates $p < 0.001$, ns indicates no significance.

including NLRP3 inflammasomes initiates pyroptosis by cleaving GSDMD to form pores in the plasma membrane, leading to cell swelling and membrane rupture, finally resulting in the leakage of mature forms of IL-1β and IL-18 out of cells.[26] As a mode of programmed cell death, pyroptosis participates in the innate immune response, inhibits intracellular pathogen replications, and activates immune cells to phagocytize and kill pathogens.[27] Once pyroptosis is out of control, inflammatory reactions are activated in adjacent cells and tissues, which further aggravates the inflammatory injury, leading to a systemic inflammatory reaction, and eventually causing organ failure or septic shock.[28] M1 polarization and pyroptosis can be activated by the same signaling pathway, including NF-kB/NLPR3 and RIG-I/Caspase1/GSDMD.[29,30] Inhibition of pro-inflammatory macrophage polarization and pyroptosis has proven to be an effective strategy for the treatment of sepsis.[31] In this study, IL-30 deficiency aggravated sepsis-induced cardiac dysfunction and

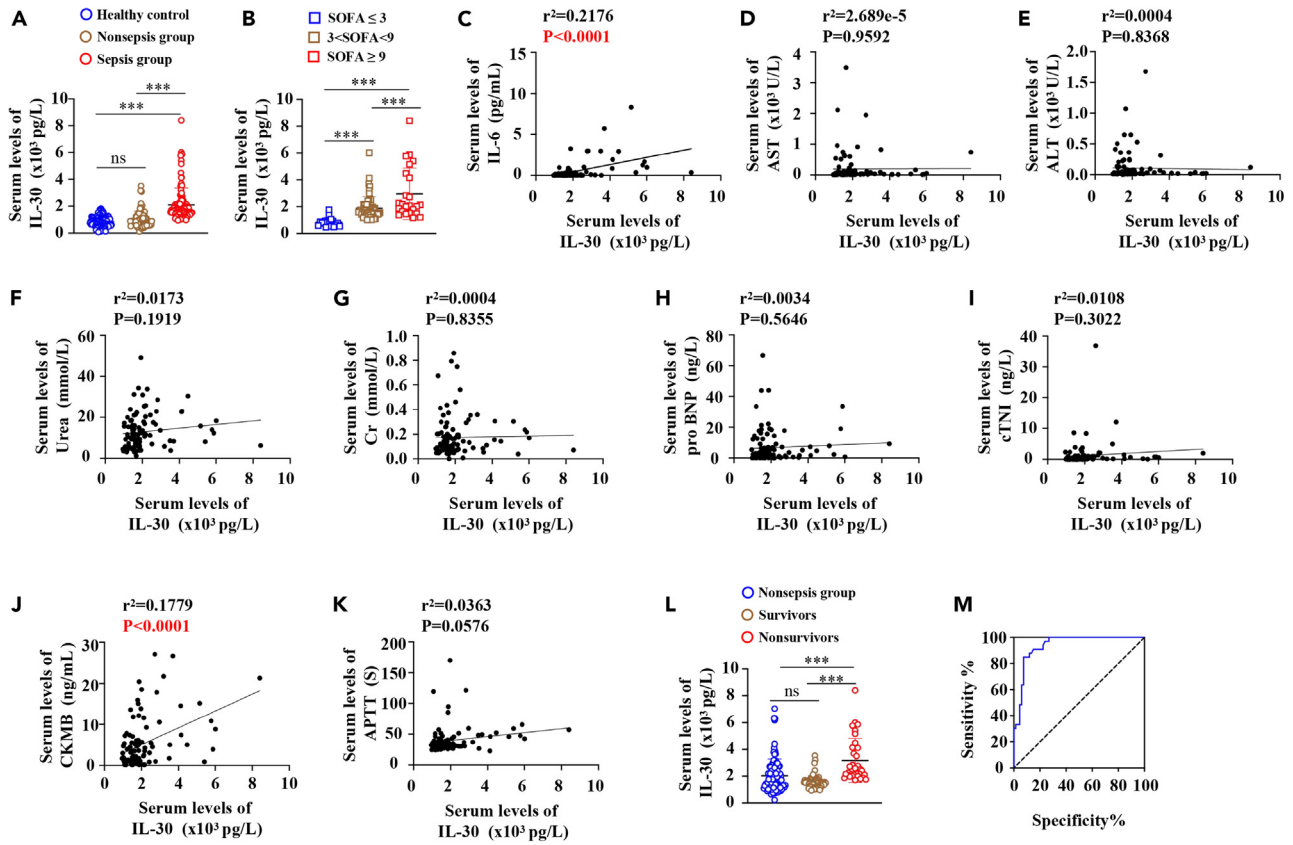

Figure 8. IL-30 in sepsis patients

(A) Serum levels of IL-30 in healthy controls (n = 100), non-sepsis patients (n = 100) and sepsis patients (n = 100).

(B) Serum levels of IL-30 in sepsis patients with different SOFA scores.

(C–K) Correlations of IL-30 levels and IL-6, AST, ALT, urea, creatinine, pro BNP, cTNI, CK-MB and APTT levels in sepsis patients.

(L) Serum levels of IL-30 in survivor, non-survivor sepsis patients and non-sepsis patients.

(M) The predictive value of IL-30 at the survivor and non-survivor of sepsis patients. An ROC curve was calculated comparing IL-30 in survivors with non-survivors. * indicates $p < 0.05$, ** indicates $p < 0.01$, *** indicates $p < 0.001$, ns indicates no significance. IL-30, interleukin 30; SOFA, sequential organ failure assessment; IL6, interleukin-6; APTT, activated partial thromboplastin time; AST, aspartate aminotransferase; ALT, alanine aminotransferase; Cr, creatinine; pro BNP, pro-brain natriuretic peptide; cTnI, cardiac troponin I; CK-MB, creatinine kinase-myocardial band.

injury by promoting Ly6C^{high} macrophage polarization and pyroptosis. NLRP3 has been reported to promote M1 macrophage polarization and pyroptosis.[30,32] In our study, the protective role of IL-30 may be associated with reduced expression of NLRP3. MCC950, a selective inhibitor of NLRP3, suppressed IL-30 deficiency-induced Ly6C^{high} macrophages polarization and pyroptosis.[12] In addition, we found that the phosphorylation level of P65 was down-regulated in IL-30 treated macrophages with LPS. P65 has been reported to regulate the activation of NLRP3 inflammasome.[33] The protective role of IL-30 may be attributed to inhibition of P65/NLRP3 signaling, which need further exploration.

In this study, we found that IL-30 KO aggravated SIMD mainly by affecting IL-30 levels but not IL-27. Recombinant IL-27 aggravated sepsis induced cardiac inflammation in IL-30 KO mice, which is consistent with previous reports.[34,35] IL-30 treatment significantly attenuated sepsis-induced cardiac dysfunction and injury. It is clear that patients with sepsis may exhibit severe comorbidities and mortality, which pose a major threat to global health. In fact, clinical studies may be the most effective way to test the clinical value of IL-30. Thus, in a cohort of sepsis patients, non-sepsis patients, and healthy controls, we found that IL-30 plasma levels were significantly elevated in sepsis patients. Significantly elevated plasma levels of IL-30 in sepsis patients were associated with IL-6, CK-MB levels, high SOFA scores, and prognosis. IL-30 can be a valid predictor of mortality in sepsis patients. During sepsis, the body produces large amounts of pro-inflammatory factors, such as IL-6 and IL-1β, which trigger an inflammatory response and cascade. Anti-inflammatory cytokines can antagonize inflammatory mediators and inhibit the development of inflammation, mainly including

IL-10, transforming growth factor β (TGF-β) and so on. When an inflammatory response occurs in sepsis patients, negative feedback increases the concentration of anti-inflammatory cytokines, which inhibits the production and release of pro-inflammatory mediators, thereby inhibiting monocyte/macrophage-related inflammation. In patients with sepsis, an imbalance of pro-inflammatory and anti-inflammatory cytokines is frequently observed. If these levels are not controlled, inflammatory cells cannot be activated effectively and cannot produce sufficient levels of anti-inflammatory cytokines. The body is prone to immune dysfunction, which can lead to the progression of sepsis. Our study shows that IL-30 is a potent anti-inflammatory cytokine. The increased expression of IL-30 in sepsis patients may be due to the negative feedback effect of the body. Our results also showed that serum IL-30 and IL-6 levels were positively correlated in the correlation analysis, suggesting a critical role of IL-30 in sepsis. Future development of kits using IL-30 as an indicator may help improve the prognosis of sepsis patients. Clinical experiments of recombinant IL-30 may help us to further confirm the clinical value of IL-30 in the treatment of sepsis.

In conclusion, IL-30 protects against SIMD by inhibiting pro-inflammatory macrophage polarization and pyroptosis. Our data provide evidence that IL-30 may be an attractive target for the treatment of SIMD.

Limitations of the study

This research still has some limitations. First, IL-30 is mainly expressed in macrophages and T lymphocytes. We only explored the effect of IL-30 on sepsis-induced macrophage polarization in this study. The effect of IL-30 on T lymphocytes needs to be further explored. Second, macrophage-specific IL-30 knockout mice may help us further explore the role of IL-30 in SIMD. Third, inhibiting P65 signal may help us further understand the protective role of IL-30.

STAR★METHODS

Detailed methods are provided in the online version of this paper and include the following:

- KEY RESOURCES TABLE
- RESOURCE AVAILABILITY
  - Lead contact
  - Materials availability
  - Data and code availability
- EXPERIMENTAL MODEL AND SUBJECT DETAILS
  - Human serum sample collection
  - Animals and animal models
  - Cell culture and treatment
- METHOD DETAILS
  - Echocardiography
  - Histological analysis
  - Biochemical determination
  - Determination of protein content in bronchoalveolar lavage fluid
  - Flow cytometry
  - Western blotting
  - Real-time quantitative PCR
- QUANTIFICATION AND STATISTICAL ANALYSIS

SUPPLEMENTAL INFORMATION

Supplemental information can be found online at https://doi.org/10.1016/j.isci.2023.107544.

ACKNOWLEDGMENTS

We acknowledge the financial support of the National Natural Science Foundation of China (82070436).

AUTHOR CONTRIBUTIONS

M.Z. was responsible for the experimental design and wrote the manuscript. P.Z. helped to collect the plasma of patients in this study. Z.Z. contributed to the western blots and qPCR. W.P. contributed to the analysis of human bioinformatics. Z.Y. contributed to the graphical abstract. J.Z., S.P., J.L., Y.X., S.X., and C.W. contributed to the acquisition and analysis of the data. J.W. and M.W. reviewed this manuscript.

DECLARATION OF INTERESTS

The authors declare that they have no known competing financial interests or personal relationships that could have appeared to influence the work reported in this paper.

Received: May 13, 2023
Revised: June 19, 2023
Accepted: August 1, 2023
Published: August 5, 2023

REFERENCES

1. Singer, M., Deutschman, C.S., Seymour, C.W., Shankar-Hari, M., Annane, D., Bauer, M., Bellomo, R., Bernard, G.R., Chiche, J.D., Coopersmith, C.M., et al. (2016). The Third International Consensus Definitions for Sepsis and Septic Shock (Sepsis-3). JAMA *315*, 801–810. https://doi.org/10.1001/jama.2016.0287.

2. Conway-Morris, A., Wilson, J., and Shankar-Hari, M. (2018). Immune Activation in Sepsis. Crit. Care Clin. *34*, 29–42. https://doi.org/10.1016/j.ccc.2017.08.002.

3. Chaudhry, H., Zhou, J., Zhong, Y., Ali, M.M., McGuire, F., Nagarkatti, P.S., and Nagarkatti, M. (2013). Role of cytokines as a double-edged sword in sepsis. In Vivo *27*, 669–684.

4. Tanaka, T., Narazaki, M., and Kishimoto, T. (2016). Immunotherapeutic implications of IL-6 blockade for cytokine storm. Immunotherapy *8*, 959–970. https://doi.org/10.2217/imt-2016-0020.

5. Yoshida, H., and Hunter, C.A. (2015). The immunobiology of interleukin-27. Annu. Rev. Immunol. *33*, 417–443. https://doi.org/10.1146/annurev-immunol-032414-112134.

6. Min, B., Kim, D., and Feige, M.J. (2021). IL-30(†) (IL-27A): a familiar stranger in immunity, inflammation, and cancer. Exp. Mol. Med. *53*, 823–834. https://doi.org/10.1038/s12276-021-00630-x.

7. Dibra, D., Cutrera, J., Xia, X., Kallakury, B., Mishra, L., and Li, S. (2012). Interleukin-30: a novel antiinflammatory cytokine candidate for prevention and treatment of inflammatory cytokine-induced liver injury. Hepatology *55*, 1204–1214. https://doi.org/10.1002/hep.24814.

8. Yan, J., Mitra, A., Hu, J., Cutrera, J.J., Xia, X., Doetschman, T., Gagea, M., Mishra, L., and Li, S. (2016). Interleukin-30 (IL27p28) alleviates experimental sepsis by modulating cytokine profile in NKT cells. J. Hepatol. *64*, 1128–1136. https://doi.org/10.1016/j.jhep.2015.12.020.

9. Mitra, A., Satelli, A., Yan, J., Xueqing, X., Gagea, M., Hunter, C.A., Mishra, L., and Li, S. (2014). IL-30 (IL27p28) attenuates liver fibrosis through inducing NKG2D-rae1 interaction between NKT and activated hepatic stellate cells in mice. Hepatology *60*, 2027–2039. https://doi.org/10.1002/hep.27392.

10. Chong, W.P., Horai, R., Mattapallil, M.J., Silver, P.B., Chen, J., Zhou, R., Sergeev, Y., Villasmil, R., Chan, C.C., and Caspi, R.R. (2014). IL-27p28 inhibits central nervous system autoimmunity by concurrently antagonizing Th1 and Th17 responses. J. Autoimmun. *50*, 12–22. https://doi.org/10.1016/j.jaut.2013.08.003.

11. Liu, X., Hu, Z., Zhang, J., Ma, T., Wu, W., Wei, X., Wang, Z., Zhen, H., Zhou, H., Huang, N., and Li, J. (2021). IL-30 ameliorates imiquimod and K14-VEGF induced psoriasis-like disease by inhibiting both innate and adaptive immunity disorders. Biochem. Biophys. Res. Commun. *579*, 97–104. https://doi.org/10.1016/j.bbrc.2021.09.042.

12. Li, H., Guan, Y., Liang, B., Ding, P., Hou, X., Wei, W., and Ma, Y. (2022). Therapeutic potential of MCC950, a specific inhibitor of NLRP3 inflammasome. Eur. J. Pharmacol. *928*, 175091. https://doi.org/10.1016/j.ejphar.2022.175091.

13. Bosmann, M., Strobl, B., Kichler, N., Rigler, D., Grailer, J.J., Pache, F., Murray, P.J., Müller, M., and Ward, P.A. (2014). Tyrosine kinase 2 promotes sepsis-associated lethality by facilitating production of interleukin-27. J. Leukoc. Biol. *96*, 123–131. https://doi.org/10.1189/jlb.3A1013-541R.

14. Bosmann, M., Russkamp, N.F., Strobl, B., Roewe, J., Balouzian, L., Pache, F., Radsak, M.P., van Rooijen, N., Zetoune, F.S., Sarma, J.V., et al. (2014). Interruption of macrophage-derived IL-27(p28) production by IL-10 during sepsis requires STAT3 but not SOCS3. J. Immunol. *193*, 5668–5677. https://doi.org/10.4049/jimmunol.1302280.

15. Liu, J., Guan, X., and Ma, X. (2007). Regulation of IL-27 p28 gene expression in macrophages through MyD88- and interferon-gamma-mediated pathways. J. Exp. Med. *204*, 141–152. https://doi.org/10.1084/jem.20061440.

16. Biswas, S.K., Chittezhath, M., Shalova, I.N., and Lim, J.Y. (2012). Macrophage polarization and plasticity in health and disease. Immunol. Res. *53*, 11–24. https://doi.org/10.1007/s12026-012-8291-9.

17. Funes, S.C., Rios, M., Escobar-Vera, J., and Kalergis, A.M. (2018). Implications of macrophage polarization in autoimmunity. Immunology *154*, 186–195. https://doi.org/10.1111/imm.12910.

18. Murray, P.J., and Wynn, T.A. (2011). Protective and pathogenic functions of macrophage subsets. Nat. Rev. Immunol. *11*, 723–737. https://doi.org/10.1038/nri3073.

19. Feng, L., Song, P., Zhou, H., Li, A., Ma, Y., Zhang, X., Liu, H., Xu, G., Zhou, Y., Wu, X., et al. (2014). Pentamethoxyflavanone regulates macrophage polarization and ameliorates sepsis in mice. Biochem. Pharmacol. *89*, 109–118. https://doi.org/10.1016/j.bcp.2014.02.016.

20. Chen, X., Liu, Y., Gao, Y., Shou, S., and Chai, Y. (2021). The roles of macrophage polarization in the host immune response to sepsis. Int. Immunopharmacol. *96*, 107791. https://doi.org/10.1016/j.intimp.2021.107791.

21. Chen, X.S., Wang, S.H., Liu, C.Y., Gao, Y.L., Meng, X.L., Wei, W., Shou, S.T., Liu, Y.C., and Chai, Y.F. (2022). Losartan attenuates sepsis-induced cardiomyopathy by regulating macrophage polarization via TLR4-mediated NF-κB and MAPK signaling. Pharmacol. Res. *185*, 106473. https://doi.org/10.1016/j.phrs.2022.106473.

22. Ruan, W., Ji, X., Qin, Y., Zhang, X., Wan, X., Zhu, C., Lv, C., Hu, C., Zhou, J., Lu, L., and Guo, X. (2021). Harmine Alleviated Sepsis-Induced Cardiac Dysfunction by Modulating Macrophage Polarization via the STAT/MAPK/NF-κB Pathway. Front. Cell Dev. Biol. *9*, 792257. https://doi.org/10.3389/fcell.2021.792257.

23. Wang, Z., Liu, M., Ye, D., Ye, J., Wang, M., Liu, J., Xu, Y., Zhang, J., Zhao, M., Feng, Y., et al. (2021). Il12a Deletion Aggravates Sepsis-Induced Cardiac Dysfunction by Regulating Macrophage Polarization. Front. Pharmacol. *12*, 632912. https://doi.org/10.3389/fphar.2021.632912.

24. Zhao, M., Li, C., Zhang, J., Yin, Z., Zheng, Z., Wan, J., and Wang, M. (2022). Maresin-1 and its receptors RORα/LGR6 as potential therapeutic target for respiratory diseases. Pharmacol. Res. *182*, 106337. https://doi.org/10.1016/j.phrs.2022.106337.

25. Liu, L., and Sun, B. (2019). Neutrophil pyroptosis: new perspectives on sepsis. Cell. Mol. Life Sci. *76*, 2031–2042. https://doi.org/10.1007/s00018-019-03060-1.

26. Yu, P., Zhang, X., Liu, N., Tang, L., Peng, C., and Chen, X. (2021). Pyroptosis: mechanisms and diseases. Signal Transduct. Target. Ther. *6*, 128. https://doi.org/10.1038/s41392-021-00507-5.

27. Miao, E.A., Leaf, I.A., Treuting, P.M., Mao, D.P., Dors, M., Sarkar, A., Warren, S.E., Wewers, M.D., and Aderem, A. (2010). Caspase-1-induced pyroptosis is an innate immune effector mechanism against

intracellular bacteria. Nat. Immunol. *11*, 1136–1142. https://doi.org/10.1038/ni.1960.

28. Zheng, X., Chen, W., Gong, F., Chen, Y., and Chen, E. (2021). The Role and Mechanism of Pyroptosis and Potential Therapeutic Targets in Sepsis: A Review. Front. Immunol. *12*, 711939. https://doi.org/10.3389/fimmu.2021.711939.

29. Li, N., Chen, J., Geng, C., Wang, X., Wang, Y., Sun, N., Wang, P., Han, L., Li, Z., Fan, H., et al. (2022). Myoglobin promotes macrophage polarization to M1 type and pyroptosis via the RIG-I/Caspase1/GSDMD signaling pathway in CS-AKI. Cell Death Discov. *8*, 90. https://doi.org/10.1038/s41420-022-00894-w.

30. Zhang, J., Liu, X., Wan, C., Liu, Y., Wang, Y., Meng, C., Zhang, Y., and Jiang, C. (2020). NLRP3 inflammasome mediates M1 macrophage polarization and IL-1β production in inflammatory root resorption. J. Clin. Periodontol. *47*, 451–460. https://doi.org/10.1111/jcpe.13258.

31. Jiao, Y., Zhang, T., Zhang, C., Ji, H., Tong, X., Xia, R., Wang, W., Ma, Z., and Shi, X. (2021). Exosomal miR-30d-5p of neutrophils induces M1 macrophage polarization and primes macrophage pyroptosis in sepsis-related acute lung injury. Crit. Care *25*, 356. https://doi.org/10.1186/s13054-021-03775-3.

32. Liu, T., Wang, L., Liang, P., Wang, X., Liu, Y., Cai, J., She, Y., Wang, D., Wang, Z., Guo, Z., et al. (2021). USP19 suppresses inflammation and promotes M2-like macrophage polarization by manipulating NLRP3 function via autophagy. Cell. Mol. Immunol. *18*, 2431–2442. https://doi.org/10.1038/s41423-020-00567-7.

33. Li, Z., Huang, Z., Zhang, H., Lu, J., Tian, Y., Wei, Y., Yang, Y., and Bai, L. (2021). P2X7 Receptor Induces Pyroptotic Inflammation and Cartilage Degradation in Osteoarthritis via NF-κB/NLRP3 Crosstalk. Oxid. Med. Cell. Longev. *2021*, 8868361. https://doi.org/10.1155/2021/8868361.

34. Wang, X., Liu, D., Zhang, X., Yang, L., Xia, Z., and Zhang, Q. (2022). Exosomes from adipose-derived mesenchymal stem cells alleviate sepsis-induced lung injury in mice by inhibiting the secretion of IL-27 in macrophages. Cell Death Discov. *8*, 18. https://doi.org/10.1038/s41420-021-00785-6.

35. Fan, J., Zhang, Y.C., Zheng, D.F., Zhang, M., Liu, H., He, M., and Wu, Z.J. (2020). IL-27 is elevated in sepsis with acute hepatic injury and promotes hepatic damage and inflammation in the CLP model. Cytokine *127*, 154936. https://doi.org/10.1016/j.cyto.2019.154936.

36. Zeng, X., Liu, G., Peng, W., He, J., Cai, C., Xiong, W., Chen, S., Yang, M., and Dong, Z. (2020). Combined deficiency of SLAMF8 and SLAMF9 prevents endotoxin-induced liver inflammation by downregulating TLR4 expression on macrophages. Cell. Mol. Immunol. *17*, 153–162. https://doi.org/10.1038/s41423-018-0191-z.

37. Ye, J., Wang, Y., Xu, Y., Wang, Z., Liu, L., Wang, M., Ye, D., Zhang, J., Yang, Z., Lin, Y., et al. (2020). Interleukin-22 deficiency alleviates doxorubicin-induced oxidative stress and cardiac injury via the p38 MAPK/macrophage/Fizz3 axis in mice. Redox Biol. *36*, 101636. https://doi.org/10.1016/j.redox.2020.101636.

38. Zhao, M., Zhang, J., Xu, Y., Liu, J., Ye, J., Wang, Z., Ye, D., Feng, Y., Xu, S., Pan, W., et al. (2021). Selective Inhibition of NLRP3 Inflammasome Reverses Pressure Overload-Induced Pathological Cardiac Remodeling by Attenuating Hypertrophy, Fibrosis, and Inflammation. Int. Immunopharmacol. *99*, 108046. https://doi.org/10.1016/j.intimp.2021.108046.

39. Wang, M., Zhao, M., Zheng, Z., Pan, W., Zhang, J., Yin, Z., Wei, C., Xu, Y., and Wan, J. (2023). TRPA1 deficiency aggravates dilated cardiomyopathy by promoting S100A8 expression to induce M1 macrophage polarization in rats. Faseb j *37*, e22982. https://doi.org/10.1096/fj.202202079RR.

40. Petes, C., Wynick, C., Guzzo, C., Mehta, D., Logan, S., Banfield, B.W., Basta, S., Cooper, A., and Gee, K. (2017). IL-27 enhances LPS-induced IL-1β in human monocytes and murine macrophages. J. Leukoc. Biol. *102*, 83–94. https://doi.org/10.1189/jlb.3A0316-098R.

41. Zhang, J., Wang, M., Ye, J., Liu, J., Xu, Y., Wang, Z., Ye, D., Zhao, M., and Wan, J. (2020). The Anti-inflammatory Mediator Resolvin E1 Protects Mice Against Lipopolysaccharide-Induced Heart Injury. Front. Pharmacol. *11*, 203. https://doi.org/10.3389/fphar.2020.00203.

STAR★METHODS

KEY RESOURCES TABLE

REAGENT or RESOURCE	SOURCE	IDENTIFIER
Antibodies		
IL-30	R&D Systems	Cat#AF1834
BAX	Abcam	Cat#ab32503
BCL2	Abcam	Cat#ab196495
Jak2	Abcam	Cat#ab108596
Jak1	Abcam	Cat#ab133666
Phospho-NF-kB p65 (S276)	Abcam	Cat#ab194726
NF-kB p65	Abcam	Cat#ab16502
Phospho-Jak1(Tyr1034/1035)	CST	Cat#74129
Phospho-Jak2 (Tyr1007/1008)	CST	Cat#66245
Phospho-Stat1 (Tyr701)	CST	Cat#9167
Stat1	CST	Cat#14994
Stat3	CST	Cat#12640
Phospho-p38 MAPK (Thr180/Tyr182)	CST	Cat#4511
p38 MAPK	CST	Cat#8690
Phospho-p44/42 MAPK (Erk1/2) (Thr202/ Tyr204)	CST	Cat#4370
p44/42 MAPK (Erk1/2)	CST	Cat#4695
Phospho-SAPK/JNK (Thr183/Tyr185)	CST	Cat#4668
SAPK/JNK	CST	Cat#9252
GAPDH	CST	Cat#5174
Cleved caspase3	GeneTex	Cat#GTX110543
Phospho-Stat3 (Tyr705)	GeneTex	Cat#GTX118000
IL-1 beta/IL1β	Santa Cruz	Cat#SC-12742
Caspase1	Santa Cruz	Cat#SC-392736
NLRP3	Immunoway	Cat#YT5382
GSDMD	Immunoway	Cat#YT7991
IL-18	Immunoway	Cat#YN1926
Horseradish peroxidase (HRP)-coupled goat anti-mouse/rabbit IgG	Abclonal	Cat#AS063, AS064
Alexa Fluor 488- and 568-conjugated secondary antibodies	Abclonal	Cat#A11008,A11001,A110011, A11004
APC-Cy™7 Rat Anti-Mouse CD45	BD Biosciences	Cat#557659
BV605 Rat Anti-Mouse Ly-6C	BD Biosciences	Cat#563011
Fixable Viability Stain 510	BD Biosciences	Cat#564406
BB700 Armenian Hamster Anti-Mouse CD3e	BD Biosciences	Cat#566494
APC Rat Anti-Mouse F4/80	eBioscience	Cat#17-4801-82
PE-Cyanine7 Rat Anti-Mouse CD11b	eBioscience	Cat#25-0112-82
Alexa Fluor® 488 Rat Anti-Mouse IL-30	R&D Systems	Cat#IC1834G
InVivoMAb anti-mouse IL-30	Bio X Cell	Cat#BE0326
Biological samples		
Human serum sample	Renmin Hospital of Wuhan University	No. WDRY2020-K223

(*Continued on next page*)

Continued

REAGENT or RESOURCE	SOURCE	IDENTIFIER
Mouse heart, lung, liver, kidney and serum	This paper	N/A
Chemicals, peptides, and recombinant proteins		
Recombinant Mouse IL-30 Protein	R&D Systems	Cat# 7430-ML
Recombinant Mouse IL-27 Protein	R&D Systems	Cat# 2799-ML
Recombinant Mouse M-CSF Protein	R&D Systems	Cat#416-ML
MCC950	Sigma	Cat# 256373-96-3
DAPI	Sigma	Cat#S7113
LPS	Sigma	Cat# L2880
FBS	Gibco	Cat#10099-141
RPMI-1640	Gibco	Cat# 11875119
Clodronate liposomes	Yeasen Biotechnology	Cat#40337ES08
TRIzol	Invitrogen	Cat#15596-026
Critical commercial assays		
Bicinchoninic acid protein assay kit	Beyotime Biotechnology	Cat#P0009
AST assay kit	Jiancheng Bioengineer	Cat#C010-2-1
ALT assay kit	Jiancheng Bioengineer	Cat#C009-2-1
CK-MB assay kit	Jiancheng Bioengineer	Cat#H197-1-1
LDH assay kit	Jiancheng Bioengineer	Cat#A020-2-2
Urea assay kit	Jiancheng Bioengineer	Cat#C013-2-1
Creatinine assay kit	Jiancheng Bioengineer	Cat#C011-2-1
cDNA synthesis kit	Basel	Cat#489703001
Human IL-30 DuoSet ELISA	R&D Systems	Cat#DY2526
Experimental models: Cell lines		
Bone marrow-derived macrophages	This paper	N/A
Experimental models: Organisms/strains		
Mouse: C57BL/6JGpt	Gempharmatech Co., Ltd	Cat#N000295
Mouse: IL-30 knockout	Gempharmatech Co., Ltd	Cat#T005558
Oligonucleotides		
Primers for PCR, see Table S3	Sangon	N/A
Software and algorithms		
MyLab 30 CV ultrasound system	Esaote S.P. A	N/A
CytExpert	Beckman	N/A
ImageJ	NIH	N/A
Image-Pro Plus	Media Cybernetics	N/A
Image Lab	Bio-Rad Laboratories	N/A
LightCycler 480 system	Roche	N/A
SPSS	IBM	N/A

RESOURCE AVAILABILITY

Lead contact

Further information and requests for resources and reagents should be directed to and will be fulfilled by the lead contact, Jun Wan (wanjun@whu.edu.cn).

Materials availability

This study did not generate new unique reagents.

Data and code availability

- All data reported in this paper will be shared by the lead contact upon request.
- This paper does not report original code.
- Any additional information required to reanalyze the data reported in this paper is available from the lead contact upon request.

EXPERIMENTAL MODEL AND SUBJECT DETAILS

Human serum sample collection

This study was approved by the Ethics Committee of the Renmin Hospital of Wuhan University (approval number: WDRY2020-K223). We recruited a total of 300 subjects from the People's Hospital of Wuhan University from July 2020 to March 2021, including 100 patients in the sepsis group, 100 patients in the non-sepsis group, and 100 subjects in the healthy control group. The inclusion criteria for the sepsis group were SOFA $\geq$ 2 with definite infection. We excluded patients under 18 years old patients who were pregnant and patients who had concurrent tumors and organ dysfunction. Sepsis patients were divided into a survival group and a deceased group according to their survival status at 28 days after admission. The non-sepsis group included patients with inflammatory infection who were not diagnosed with sepsis, and the exclusion criteria were the same as those in the sepsis group. The control group included healthy subjects who went to the hospital for physical examination during the same period, excluding subjects who were under 18 years old, had organ dysfunction, had signs of infection in the previous month, or received antibiotics or other nonprophylactic drugs for other reasons. The serum levels of IL-30 (R&D Systems, DY-2526) were detected according to the manufacturer's instructions. The influence of sex and age was analysed and results are shown in Table S2.

Animals and animal models

IL-30 knockout (KO) mice on the C57BL/6 background were purchased from the Institute of Model Animals, Nanjing University (imported from the Jackson Laboratory). Wild-type (WT) mice in the same brood were used as controls. All animals were housed at constant room temperature on a 12:12 hours light-dark cycle at the Animal Center of Wuhan University Renmin Hospital and fed a standard rodent diet and water. Male KO mice and WT mice at 10 weeks of age were used in this study. All animals received humane care according to NIH (USA) guidelines. All animal care and experimental procedures were approved by the Animal Policy and Welfare Committee of Wuhan University Renmin Hospital (approval number: WDRM20210603).

The CLP mouse model was prepared as previously described.[23] Mice were anesthetized with ketamine (50 mg/kg) and xylazine (5 mg/kg) via i.p. injection. After disinfection, a 1 cm midline laparotomy was made in the abdomen. The cecum was then exteriorized, and ligated below the cecal valve, and punctured with an 18-gauge needle to induce sepsis. A small drop of cecal content was extruded. The cecum was then returned to the peritoneal cavity and the abdominal incision closed with sutures. Mice were resuscitated with (5 ml/100 g) saline. Sham animals underwent the same surgical procedures without cecum ligation and puncture. At 24 hours after surgery, the animals were euthanized with phenobarbital overdose (100 mg/kg body weight), followed by collection of the heart tissues as described previously.

To examine the role of IL-30 neutralization in sepsis mice, a neutralizing polyclonal antibody against IL-30 (40 mg/mouse, i.p.) or control IgG (40 mg/mouse, i.p.) was injected twice at 24 hours and 1 hour before CLP for preventive treatment.[14]

To explore the role of bone marrow cell-derived IL-30 in SIMD, clodronate liposomes (CL) (200 μl per mouse) was first injected once two days before CLP.[36] Bone marrow cells were then extracted from WT mice and IL-30 KO mice and reinfused into WT mice via tail vein injection at 24 hours before CLP.[37]

To examine the role of IL-30 and IL-27 in sepsis mice, recombinant IL-30 (1 μg per mouse), IL-27 protein (1 μg per mouse) or control vehicle (PBS) was injected twice at 24 hours and 1 hour before CLP for preventive treatment.[8]

To examine the role of pyroptosis in mice with sepsis, MCC950 (10mg/kg body weight) or control vehicle (PBS) was injected twice at 24 hours and 1 hour before CLP.[38]

Cell culture and treatment

Bone marrow-derived macrophages (BMDMs) were obtained from WT and KO mice as previously described.[39] Briefly, after euthanasia of WT and KO mice, tibias and femurs were isolated. Then, the bone marrow cavity was exposed and washed with RPMI 1640 medium to obtain a cell suspension. After the cell suspension was filtered, erythrocytes were lysed and washed, the target bone marrow cells were resuspended in 10% FBS (RPMI 1640 medium containing 1% penicillin/streptomycin). Then, M-CSF (20 ng/ml) was used for one week to allow BMDMs to differentiate. Differentiated BMDMs were treated with LPS (100 ng/ml) to induce M1 macrophage polarization. After 12 hours of stimulation, cultured cells were used for further analysis.

To investigate the role of NLRP3 (NOD-like receptor thermal protein domain associated protein 3) in IL-30 deficiency induced macrophage polarization and pyroptosis, MCC950 (7.5 nM) was given 0.5 h before stimulation with LPS. To examine the role of IL-30 in BMDMs, IL-30 (100 ng/ml) was added to the medium 0.5 hour before LPS challenge.[40]

METHOD DETAILS

Echocardiography

Systolic and diastolic cardiac function in anesthetized mice was measured noninvasively by transthoracic echocardiography 15 minutes before sacrifice as described.[38] Mice were anesthetized with isoflurane using 1.5% isoflurane, and the ventricular septum, chamber dimensions, systolic and diastolic function, and ejection fraction were recorded by a MyLab 30 CV ultrasound system (Esaote S.P. A, Genoa, Italy).

Histological analysis

The lung samples were isolated and fixed with 4% paraformaldehyde for 48 h and then dehydrated by ethanol solution with different concentrations (70%-100%) for 40 min. Following paraffin embedding, the samples were preserved for the subsequent experiments. The sections were sliced into 4 μm sections and placed in xylene, anhydrous ethanol, and alcohol to dewax in sequence. Hematoxylin-eosin (HE) was utilized to stain the lung samples. The slides were dyed with hematoxylin for 5 min and rinsed with water, and then after returning to blue, the slides were stained with eosin for 1-3 min. The degree of lung damage was assessed by two independent technicians. The scores were recorded according to the degree of neutrophil infiltration, alveolar and interstitial edema, and hemorrhage in lung tissues. The range of scores was from 0 to 4: 0, normal lung; 1, mild lung injury (less than 25% injury); 2, moderate lung injury (25%-50% injury); 3, broad lung injury (50%-75% injury); and 4, extreme lung injury (more than 75% injury). The individual scores of each criterion were added and calculated as the final lung injury score. The histological photographs were observed by optical microscopy (Nikon, Japan).

For immunofluorescence staining, harvested mice hearts were embedded in paraffin and cut into 5-micron thick sections. Sections were incubated with primary antibodies against IL-30, F4/80 and caspase1 overnight in a humidified chamber at 4°C. Sections were then incubated with secondary antibody for 1 hour in the dark. Sections were evaluated using a fluorescence microscope (Olympus DX51, Tokyo, Japan) and further analyzed using Image-Pro Plus software (version 6.0).

Biochemical determination

Blood samples were centrifuged at 4000 rpm for 15 minutes immediately after collection, and then the supernatant serum was collected and stored at -80°C until subsequent analysis. Cardiac tissue was triturated in phosphate buffered saline to obtain tissue homogenate. Serum levels of urea, creatinine, AST, ALT, serum and cardiac tissue concentrations of CK-MB and LDH were detected with reagent test kits (Jiancheng Bioengineer, China) according to the manufacturer's instructions.

Determination of protein content in bronchoalveolar lavage fluid

BALF was obtained from the left lung post-experiment. Following the manufacturer's protocol, mice were euthanized and fixed, the skin was incised in the middle of the neck, the trachea was separated, and the right bronchi was ligated. The left bronchus was punctured with a fine needle and fixed with silk thread. Then, 0.5 ml of PBS was injected into the bronchi, and the BALF was slowly recovered after 1 min. Repeat the above operation five times. The collected BALF was centrifuged at 1500 rpm for 10 min at 4°C, and the

supernatant was recovered and stored at -20°C for protein concentration determination. The content of protein was checked by the commercial bicinchoninic acid protein assay kit (Beyotime, China).

Flow cytometry

Flow cytometry was used to analyze mice cardiac tissue as described in our previous study.[41] In brief, left ventricular tissue was digested with 0.1% collagenase II and 2.4 U/ml dispase II to prepare a single-cell suspension. To examine the BMDMs, cells in culture dishes were digested with 0.25% trypsin in culture dishes to prepare RAW cell suspensions. Then, primary antibodies were used for flow cytometry, including CD45, IL-30, CD11b, F4/80, Ly6C and CD3. After the primary antibodies were incubated for 30 min in the dark, the cells were analyzed with CytExpert (Beckman, USA) or MoFlo XDP (Beckman, USA).

Western blotting

After protein extraction from mouse cardiac tissue, Western blotting was performed as previously described.[23] Briefly, protein samples (50 μg) were separated by 10% SDS–PAGE and subsequently transferred to PVDF membranes (FL00010, Millipore, Billerica, MA, USA). PVDF membranes were blocked with 5% nonfat milk for 1 h at room temperature to block nonspecific binding sites and then incubated with primary antibody overnight at 4°C. The protein expression level of GAPDH was used as an internal standard. The next day, the membranes were incubated with the secondary antibody for 1 hour at room temperature. Finally, blots were obtained and scanned by Image Lab software (Bio-Rad Laboratories, Inc., Hercules, CA, USA) to assess protein expression.

Real-time quantitative PCR

Cells or cardiac tissues were homogenized in TRIzol (15596-026, Invitrogen Corporation, Waltham, MA, USA), followed by a cDNA synthesis kit (489703001, Basel, Switzerland) reverse transcription of mRNA into complementary DNA (cDNA). The LightCycler 480 system (04896866001, Roche) was used for qPCR analysis. Primers for target genes are listed in Table S3. The amount of each gene was determined and normalized to the amount of GAPDH.

QUANTIFICATION AND STATISTICAL ANALYSIS

All the data in this study were expressed as the mean ± standard error of the mean (SEM) and analyzed using the SPSS 23.0 software. Unpaired Student's t test was used for comparisons between two groups. Two-way analysis of variance (ANOVA) without repeated measures was performed for multiple comparisons with two independent variables. One-way ANOVA with Tukeys post hoc test was used for comparisons among three or more groups. Tukey's tests were run only when F achieved $p < 0.05$, and no significant variance inhomogeneity was found; otherwise, Tamhane's T2 post hoc test was performed. Normality and homogeneity were tested using Liljefors' and Levene's tests, respectively. Statistical significance was set at $p < 0.05$.